

Exploration of electronic quadrupole states in atomic clusters by two-photon processes

V.O. Nesterenko¹, P.-G. Reinhard², T. Halfmann³, and E. Suraud⁴

¹*Laboratory of Theoretical Physics, Joint Institute for Nuclear Research,
Dubna, Moscow region, 141980, Russia**

²*Institute of Theoretical Physics II,
University of Erlangen-Nurnberg, D-91058, Erlangen, Germany*

³*Department of Physics, Technical University Kaiserslautern, D-67653, Germany*

⁴*Institute of Electronics, Bulgarian Academy of Sciences, Sophia, Bulgaria and*

⁴*Laboratoire de Physique Quantique, Université Paul Sabatier,
118 Route de Narbonne, 31062 cedex, Toulouse, France*

(Dated: July 6, 2018)

Abstract

We analyze particular two-photon processes as possible means to explore electronic quadrupole states in free small deformed atomic clusters. The analysis is done in the time-dependent local density approximation (TDLDA). It is shown that the direct two-photon population (DTP) and off-resonant stimulated Raman (ORSR) scattering can be effectively used for excitation of the quadrupole states in high-frequency (quadrupole plasmon) and low-frequency (infrared) regions, respectively. In ORSR, isolated dipole particle-hole states as well as the tail of the dipole plasmon can serve as an intermediate state. A simultaneous study of low- and high-frequency quadrupoles, combining DTP and ORSR, is most effective. Femtosecond pulses with intensities $I = 2 \cdot 10^{10} - 2 \cdot 10^{11} W/cm^2$ and pulse durations $T = 200 - 500$ fs are found to be optimal. Since the low-lying quadrupole states are dominated by one single electron-hole pair, their energies, being combined with the photoelectron data for hole states, allow to get the electron spectrum above the Fermi level and thus greatly extend our knowledge on the single particle spectra of clusters. Besides, the developed schemes allow to estimate the lifetime of the quadrupole states.

*Electronic address: nester@theor.jinr.ru

I. INTRODUCTION

In recent years, the achievements in laser technologies have lead to a remarkable progress in the analysis of electronic degrees of freedom in atomic clusters, for an extensive review see [1]. For example, photoelectron spectra (PES) can now be measured with a high accuracy and for a broad variety of clusters [2, 3, 4, 5, 6, 7, 8]. However, a wealth of electronic modes still remains unexplored. In clusters with the diameter far below the laser wavelength (i.e. in clusters with the number of atoms $N < 10^6 - 10^8$), the laser light couples only to dipole ($\lambda = 1$) states. Hence we gain the well known dipole plasmon. At the same time, it is still very hard to access the electronic modes with higher multipolarity $\lambda > 1$. Multi-photon processes can generally give a way to these modes. For example, two photons couple to quadrupole ($\lambda = 2$) modes [9]. Just this case, investigation of quadrupole modes of valence electrons in two-photon processes, will be scrutinized in the present paper. In a previous publication [10], we have studied the scenario of two-photon processes where both photons originate from the same laser pulse and so have the same frequency. In this paper, we will analyze an alternative two-photon technique employing two different laser frequencies. It will be shown that the combined implementation of both techniques is most optimal for the exploration of electronic quadrupole states.

A particularly interesting aspect emerges for low-frequency (infrared) quadrupole modes in small deformed clusters. It was found that these modes are dominated by a single electron-hole (1eh) pair [9, 10] and their spectra are close to the pure 1eh energy differences $\epsilon_{eh} = \epsilon_e - \epsilon_h$. As a result, measuring the energy ϵ_{eh} in a two-photon process and the energy of the hole (occupied) state e_h by PES [2, 3, 4], we gain information on the particle energy ϵ_e . This allows to determine the full single-particle spectrum of valence electrons near the HOMO-LUMO (highest occupied molecular orbital - lowest unoccupied molecular orbital) gap. Being sensitive to diverse cluster's features (equilibrium shape, ionic structure, ...), the electronic spectra can in turn serve for investigations of these features. Besides they constitute a critical test of any theoretical description.

It is worth noting that, unlike the dipole states with their high frequencies and strong collective mixing, the quadrupole states of interest mainly originate from the deformation splitting [9, 10]. Their energy scale is thus quite small and they usually lie in the infrared region $< 1eV$. In small clusters the spectrum of these states is very dilute. This prevents

collective mixing of the states, favors their $1eh$ nature, and simplifies the experimental discrimination. Different kinds of small deformed clusters (free, supported, embedded) can be explored for the infrared quadrupole modes. In this paper we will consider the simplest case of free clusters.

Two-photon processes allow to excite not only the low-frequency quadrupole modes, but also high-frequency quadrupole states in the regime of the quadrupole plasmon. In fact, these plasmon states carry a large quadrupole strength and thus rather easily respond to two-photon probes. The two sorts of quadrupole modes can be characterized in terms of transitions between major quantum shells of the cluster mean field [9]. The low-frequency quadrupole modes correspond to $1eh$ excitations within the valence quantum shell N ($\Delta N = 0$ modes). The high-frequency states in the quadrupole-plasmon range correspond to the excitations over two major shells ($\Delta N = 2$ modes). There are still no any experimental data about both kinds of modes. But their investigation could deliver a valuable spectroscopic information.

As mentioned above, the excitation of quadrupole states needs at least a two-photon process. A variety of such processes is known in atomic and molecular spectroscopy [11, 12, 13, 14]. However, to our knowledge, none has been applied so far in experimental investigations of atomic clusters. Some of these processes, namely the direct two-photon population (DTP) [10], the off-resonant stimulated Raman scattering (ORSR) [12], and the stimulated Raman adiabatic passage (STIRAP) [13, 14], seem to be quite promising [15] and are thus worth a closer inspection. As is shown below, some particular cluster properties, e.g. high probability of undesirable plasmon population, complicates implementation of two-photon schemes. Hence we need a detailed analysis based on realistic calculations. As a first step in this direction, the pump-probe DTP method was recently investigated [10]. In this method the electronic infrared quadrupole state is generated via the direct resonant two-photon (two-dipole) excitation by the pump laser, see the DTP scheme at the left part of figure 1. The population of the quadrupole state is detected through the appearance of satellites in the photoelectron spectra produced by a probe pulse (not shown in figure 1). Femtosecond pump and probe pulses with intensities $I = 2 \cdot 10^{10} - 2 \cdot 10^{11} W/cm^2$ and pulse duration $T = 200 - 500$ fs were found to be optimal. The systematic TDLDA calculations have shown that the method is very robust and delivers not only the $1eh$ spectrum but also the lifetime of the $1eh$ pairs.



FIG. 1: Schemes of two-photon processes: direct two-photon (DTP) in a two-level system and off-resonant stimulated Raman (ORSR) in a three-level Λ -system. The initial $|0\rangle$, intermediate $|1\rangle$, and target $|2\rangle$ states have the orbital moments $\lambda = 0, 1$, and 2 , respectively. In ORSR the pump dipole pulse couples the ground and intermediate states while the Stokes dipole pulse provides the coupling of the intermediate and target states. Δ is the detuning from the intermediate dipole state $|1\rangle$. The purpose of both DTP and ORSR is the population of the target quadrupole state $|2\rangle$.

In the present paper, we aim to inspect an alternative two-photon method, off-resonant stimulated Raman scattering (ORSR). In this method, the target quadrupole state is populated by two different dipole transitions via an intermediate dipole state. Hence we deal with the so called Λ -system, see right part of figure 1. The pump pulse provides the coupling of the initial (ground) state $|0\rangle$ to the intermediate state $|1\rangle$. The Stokes pulse couples $|1\rangle$ with the quadrupole target state $|2\rangle$, altogether stimulating the transition to the target state. The pulses have to maintain the two-photon resonance condition $\omega_p - \omega_s = \omega_2$, i.e. the difference of the pump and Stokes frequencies must coincide with the frequency of the target quadrupole state. Isolated dipole states of $1e\hbar$ nature as well as the dipole plasmon can serve as the intermediate state $|1\rangle$. However, one should avoid a real population of the intermediate state to prevent undesirable leaking into competing channels. This is especially important for the dipole plasmon which decays via a fast Landau damping associated with a short lifetime ($\sim 10 - 20$ fs) [1]. To avoid the actual population of $|1\rangle$, we will use an appreciable detuning Δ from the energy of this state, hence the reference to *off-resonant* process. A considerable detuning is the crucial point in our scheme. Detection of the population of the target quadrupole states (both at low- and high-frequency) in the ORSR can be done by a probe pulse in the same way as in the DTP [10]. As compared with DTP, the ORSR scheme is more involved since it requires not two but three different pulses (pump, Stokes and probe). At the same time, the ORSR allows to explore the low-lying quadrupole

states by lasers in the region of visible light and hence is an interesting alternative to DTP. Besides, ORSR is widely used in atomic and molecular physics. It is certainly worth to assay this method for atomic clusters as well.

In the present study, we will apply the ORSR to low-frequency quadrupole states. However, as is shown below, it is hard to explore these states without touching the high-frequency quadrupoles which very easily respond to any two-photon probes. Both kinds of quadrupole states should thus be involved into a realistic exploration scheme. The high-frequency quadrupoles can hardly be studied within the ORSR in Λ -configuration because in this case we would need the intermediate dipole state lying above the quadrupole plasmon [24]. It is hence better to explore these quadrupoles by DTP. As a result, we naturally come to a combined analysis implementing the ORSR for the low-frequency quadrupoles and the DTP for their high-frequency counterparts. The aim of the present paper is to develop optimal schemes for the combined DTP-ORSR method.

The paper is outlined as follows. In Section 2 the calculation scheme is sketched. In Sec. 3 the ORSR excitation of the low-frequency quadrupole is discussed for two cases of the intermediate state: an isolated dipole state and tail of the dipole plasmon. Stability of the process to variation of the main parameters is scrutinized. The DTP population of the quadrupole plasmon states is outlined and the general scheme for the combined DTP-ORSR experiment is developed. The conclusions are drawn in Sec. 4.

II. CALCULATION SCHEME AND TEST CASE

The theoretical and numerical framework of our study are explained in detail elsewhere [1, 16]. So we summarize here only the key points. The calculations are performed within the time-dependent local density approximation (TDLDA) using the exchange-correlation functional of [17] and an averaged self-interaction correction [18]. As a first step, the static single-electron wave functions $\bar{\phi}_i(\vec{r})$ are calculated from the stationary Kohn-Sham equations. Then time evolution of the single-electron wave functions $\phi_i(\vec{r}, t)$ is computed starting from the initial condition $\phi_i(\vec{r}, t = 0) = \bar{\phi}_i(\vec{r})$. The ionic background is treated in the soft jellium approximation [1]. This approximation, although a bit daring, is capable of reproducing the basic trends of shapes and subsequent plasmon spectra of Na clusters [19, 20, 21]. In the present paper we consider axially deformed clusters and therefrom Na_{11}^+ as a particu-

TABLE I: The spectrum of the quadrupole states below 1 eV in Na_{11}^+ , approximated by the energies of the dominant $1eh$ pairs. The structure of $1eh$ pairs is done in terms of the Nilsson-Clemenger quantum numbers $[Nn_z\Lambda]$ [23]. See text for more details.

$\lambda\mu$	$\hbar\omega$ [eV]	$[Nn_z\Lambda]_e$	$[Nn_z\Lambda]_h$
21	0.41	[211]	[220]
22	0.60	[202]	[220]
20	0.75	[200]	[220]

larly suitable test case. The axial symmetry and jellium approximation together greatly reduce the computational effort and thus allow huge scans in the multi-parameter space of multi-photon processes even in deformed clusters. Absorbing boundary conditions are employed for the description of photoionization. The numerical handling is performed by standard methods (gradient iterations for the ground state, time splitting for time propagation). The excitation spectra in the linear response regime are computed in TDLDA by standard techniques of spectral analysis [16, 22]. The laser induced dynamics is simulated by adding to the TDLDA the laser pulses as classical external dipole fields of the form $W(t) = E_0 z \sin^2(\pi t/T) \cos(\omega t)$ with the field strength E_0 (\propto square root of the intensity I) lasting for one half-cycle of the profile function $\sin^2(\pi t/T)$. The field is applied in z -direction (the symmetry axis of the system); ω is the frequency and T is the pulse duration. Small deformed sodium clusters are optimal for a first exploratory analysis. We consider here the test case Na_{11}^+ . It is strongly prolate which provides a comfortably strong collective splitting of the plasmon resonance and of the single-electron spectrum. Its infrared spectrum below 1 eV is very dilute and displays only three well separated electronic levels, namely the quadrupole modes of multipolarity $\lambda\mu=20, 21$ and 22 (see Table 1). Following our estimations [9], these modes almost correspond to pure $1eh$ states as indicated in Table 1. The collective shifts of these states through the Coulomb residual interaction are modest, e.g. ~ 0.05 eV for $\lambda\mu=20$, which corroborates their $1eh$ structure. This feature is a direct consequence of the dilute spectrum, because large energy intervals between the levels prevent their collective mixture. In Na_{11}^+ dipole states start above 1 eV and so are well separated from the low-frequency quadrupole modes. Such a spectral separation is a general feature of small deformed clusters. As was mentioned above and as can be seen from Table 1, the

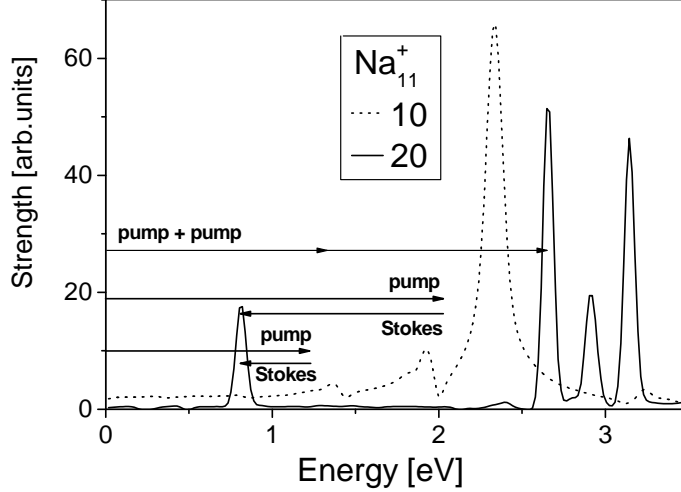


FIG. 2: Dipole ($\lambda\mu = 10$) and quadrupole ($\lambda\mu = 20$) strength distributions in Na_{11}^+ . The large peaks above 2 eV represent the states of the dipole and quadrupole plasmons. The sets of horizontal arrows depict two-photon (two-dipole) processes: DTP (pump + pump) and ORSR (pump + Stokes). The latter runs via the isolated dipole state at 1.35 eV and the tail of the dipole plasmon. The low- and high-frequency quadrupole states of interest are seen as peaks at 0.8 and 2.6 eV.

low-frequency quadrupole modes are represented by the $1eh$ transitions inside the valence shell ($\Delta N = 0$). Moreover, most of these modes arise due to the deformation splitting of the levels and so their energy scale is small. Instead, the dipole modes are generated by $\Delta N = 1$ electron-hole transitions between the neighbor quantum shells and thus acquire much higher energies. The effective energy separation of the quadrupole and dipole modes favors discrimination of the low-frequency quadrupole spectrum.

In what follows, we will concentrate on the states with $\lambda\mu=20$. This suffices for our exploration. Besides, the limitation to $\lambda\mu=20$ allows to maintain the axial symmetry which, in turn, reduces computational expense. Figure 2 shows the relevant part of the excitation spectrum in terms of the dipole ($\lambda\mu = 10$) and quadrupole ($\lambda\mu = 20$) photo-absorption strengths. The low- and high-frequency quadrupole modes of interest are seen at the energies $e_{20} = 0.8$ and 2.6 eV. The horizontal arrows depict the DTP and ORSR processes considered below. Two ORSR versions are discussed. In the first case, the process runs via the isolated dipole state at 1.35 eV. In the second case, it proceeds via the intermediate region between the isolated dipole state at 1.9 eV and the dipole plasmon. In both cases, there is an appreciable detuning from the dipole states such that one deals only with remote tails of the states.

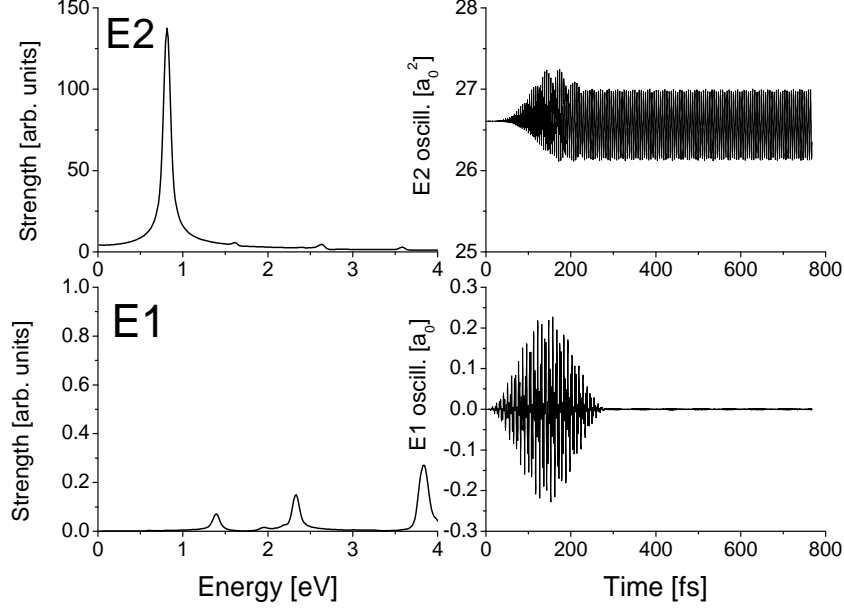


FIG. 3: ORSR in Na_{11}^+ via the isolated dipole state at 1.35 eV. The left panels show quadrupole and dipole strengths as function of the excitation energy. The right panels display the electronic quadrupole and dipole moments (in atomic units) as a function of time. It is seen that, while the quadrupole oscillation is persistent, (right-top plot), the dipole signal exists only during the coinciding pump and Stokes pulses (right-bottom plot). The calculations were performed for laser frequencies $\hbar\omega_s = 0.46$ eV and $\hbar\omega_p = 1.27$ eV, intensities $I_s = 1.5I_p = 2.2 \cdot 10^{10} \text{ W/cm}^2$ and pulse durations $T_s = T_p = 300$ fs. The detuning from the intermediate state is $\Delta \sim 0.08$ eV.

III. RESULTS AND DISCUSSION

A. ORSR for low-frequency isolated quadrupole

Figure 3 shows the ORSR via the isolated dipole state at 1.35 eV with a detuning of $\Delta \sim 0.08$ eV. The right panels show time evolution of the dipole and quadrupole moments. It is seen that the ORSR mechanism leads to *enduring* quadrupole oscillation. Since electron-ion and electron-electron relaxations are not taken into account here, these oscillations persist for several ps and further. The dipole oscillations, on the other hand, exist only during the pulses at $t = 0-300$ fs. The left panels display the corresponding dipole and quadrupole strengths in the frequency domain, obtained as the Fourier transforms of the oscillating moments. The quadrupole mode of interest at 0.81 eV dominates all other quadrupole excitations, even the quadrupole plasmon. So, just this mode is presented in the enduring

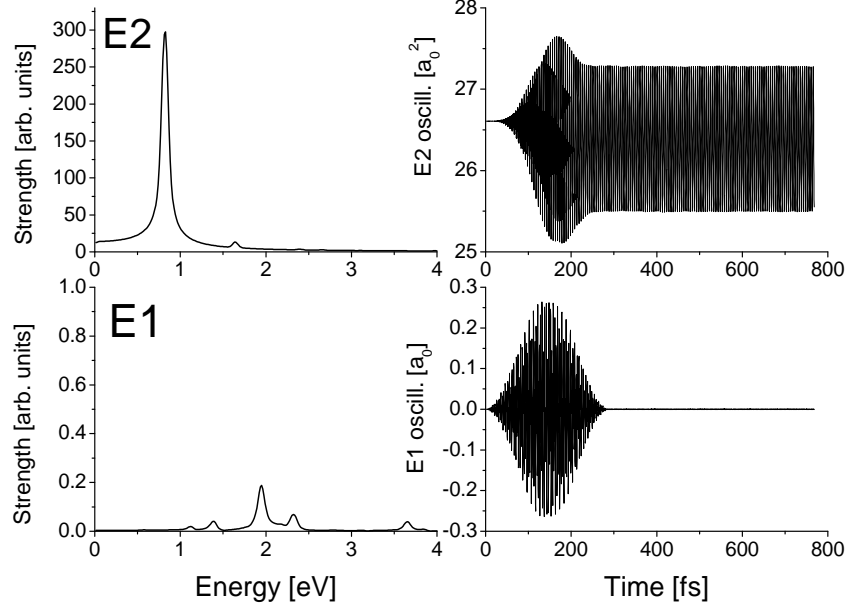


FIG. 4: Similar as figure 3 but for an intermediate dipole frequency of 2.05 eV. The calculations were performed for the laser frequencies $\hbar\omega_s = 1.24$ eV and $\hbar\omega_p = 2.05$ eV, intensities $I_s = 1.5I_p = 1.44 \cdot 10^{10} \text{W/cm}^2$ and pulse durations $T_s = T_p = 300$ fs. The detuning is $\Delta \sim 0.15$ eV with respect to the dipole state at 1.9 eV and $\Delta \sim 0.25$ eV with respect to the dipole plasmon at 2.3 eV.

oscillation seen in the right-top panel. The dipole strength is negligible (compare different scales of the top and bottom panels) and so should not noticeably compete with the quadrupole mode of interest. As was shown in [10], a significant decoupling of competing modes is crucial for detection of the target quadrupole state.

Figure 4 shows results for the ORSR via the region between two close dipole structures. The pump laser frequency 2.05 eV is placed between the isolated peak $1eh$ at 1.9 eV and the tail of the dipole plasmon lying at 2.3 eV, thus representing a considerable detuning from both dipole structures. As these structures are much stronger than the intermediate dipole in the previous case, it becomes possible to get twice larger quadrupole signal even at the lower laser intensity ($I_s = 1.5I_p = 1.44 \cdot 10^{10} \text{W/cm}^2$ against $I_s = 1.5I_p = 2.2 \cdot 10^{10} \text{W/cm}^2$ in figure 3). Like in the previous case, we have no appreciable competitors though now the pump frequency is rather close to the dipole plasmon. Altogether, figures 3 and 4 justify that one can get robust ORSR signals in clusters via both isolated dipole states and tail of the dipole plasmon.

One may observe in the right-up panel of figure 4 that the quadrupole oscillation leads to some shift of the average quadrupole moment. Indeed, the oscillation starts at the moment

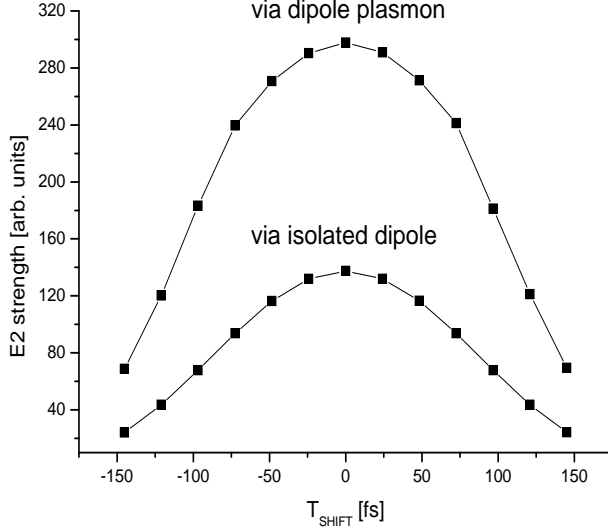


FIG. 5: The quadrupole strength as a function of the pulse shift for ORSR via the isolated dipole state and the dipole plasmon.

$26.6 a_0^2$ but then proceeds around a bit lower average value $\sim 26.4 a_0^2$. Our analysis shows that this effect is caused by a non-isotropic emission of electrons from the cluster. Indeed, the axial cluster Na_{11}^+ has a shape of the prolate ellipsoid. The quadrupole oscillation of multipolarity $\lambda\mu = 20$ drives electrons along the symmetry axis of the cluster and thus favors emission of electrons from the poles of the cluster ellipsoid. This makes the shape of the electron subsystem more spherical and therefore effectively decreases the quadrupole moment. The stronger the oscillation, the larger the moment shift. Hence the effect is most apparent in figure 4 which exhibits the strongest quadrupole mode. However, even in this case the moment shift is quite modest (2%) and thus should not noticeably influence the accuracy of measurements of the energy of the quadrupole mode in ORSR experiments.

B. Coherence and population for the target state

Figures 3 and 4 were obtained with simultaneously active pump and Stokes pulses, i.e. with the relative time shift $T_{\text{shift}} = 0$. The dependence of the quadrupole peak height on the time shift is shown in figure 5. It is seen that the maximal quadrupole strength is achieved at coincident pump and Stokes pulses. A similar picture emerges for stimulated Raman scattering, when plotting the population of the state instead of its strength [11, 12, 13]. However, such a correlation between the strength and population arises only at low

population and does not imply equality of these two characteristics. This point deserves a closer inspection.

Let us confine the formal considerations to the active subspace. At any time t , the many-body wave function of the three-level Λ system can be represented as a superposition

$$\psi(t) = c_0(t)|0\rangle + c_1(t)|1\rangle + c_2(t)|2\rangle \quad (1)$$

where $c_0(t)$, $c_1(t)$ and $c_2(t)$ are time-dependent amplitudes of the initial, intermediate and final bare states, respectively. The population of the target quadrupole state then reads $|c_2(t)|^2$. But the strength of the quadrupole transition (considered in figures 3-5) is $\sim c_0(t)*c_2(t)\langle 2|E2|0\rangle^2$ and so corresponds not to the population but to the coherence $c_0(t)*c_2(t)$ of the initial and target states. The population and coherence have different behaviors. They both grow at the onset of the population of the level $|2\rangle$ but then the coherence gets the maximum at $c_0^2(t) = c_2^2(t) = 0.5$ and begins to vanish with further increasing $|c_2(t)|^2$ from 0.5 to 1.

The calculation of the population $|c_2(t)|^2$ in TDLDA is somewhat involved. So, in the present study, we will only consider a simple estimate. We know that the dominant component of the low-frequency quadrupole state is the $1eh$ configuration $[200]_e[220]_h$ (see Table 1). To populate this configuration, the electron from the occupied state $[220]$ should be transferred to the unoccupied state $[200]$. This should manifest itself in the time dependent single-particle wave function $\phi_{[220]}(\vec{r}, t)$. Namely, it has to coincide with the initial state $\bar{\phi}_{[220]}(\vec{r})$ at $t=0$ and then acquire large contribution of $\bar{\phi}_{[200]}(\vec{r})$ in the course of time. Hence the population $P_2^{eh}(t)$ of the $[200]_e[220]_h$ quadrupole component can be estimated as the squared overlap

$$P_2^{eh}(t) = \left| \int d\vec{r} \phi_{[220]}(\vec{r}, t) \bar{\phi}_{[200]}(\vec{r}) \right|^2. \quad (2)$$

This estimate yields for $t > 600$ fs (i.e. for the time when, following figures 3 and 4, only the low-lying quadrupole mode survives) quite small population 0.01-0.03. Instead, the overlap with the initial static state

$$P_2^{in}(t) = \left| \int d\vec{r} \phi_{[220]}(\vec{r}, t) \bar{\phi}_{[220]}(\vec{r}) \right|^2 \quad (3)$$

turns out to contribute the complementing 99-97%. Similar relations were obtained for the direct two-photon (DTP) excitation of the quadrupole, described in [10]. During the

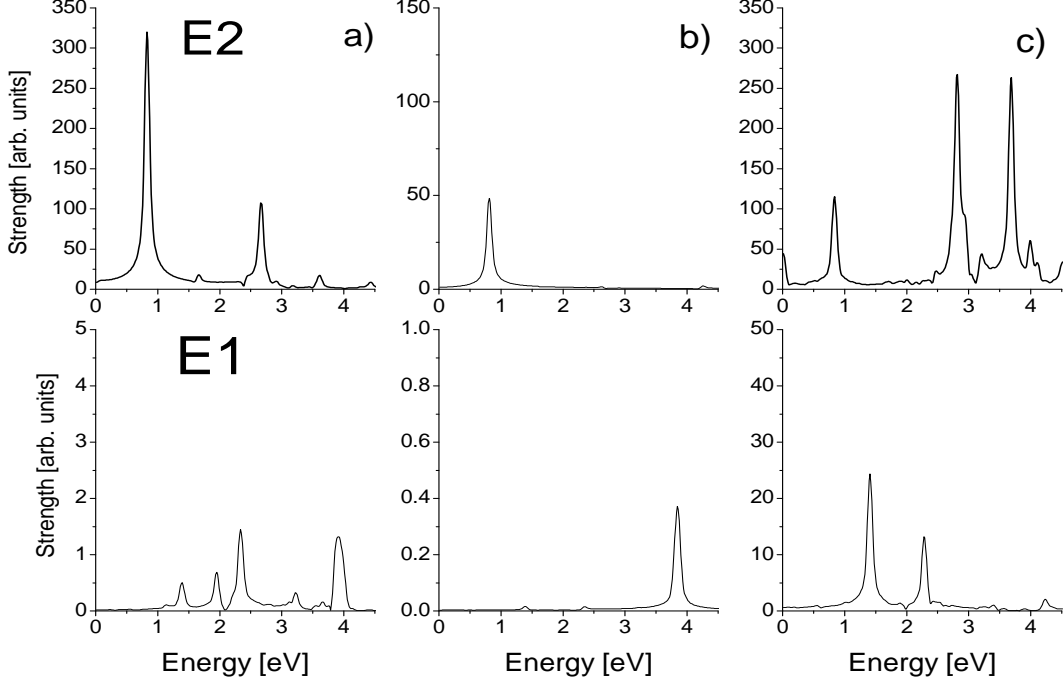


FIG. 6: The strengths calculated as in figure 3 but a) for larger intensities $I_s = 1.5I_p = 7.44 \cdot 10^{10} \text{W}/\text{cm}^2$; b) with small deviation 0.03 eV from the two-photon resonance; c) without detuning from the intermediate dipole state. See text for more details.

time evolution, the single-electron wave functions thus mainly keep their initial structure and only a small fraction (a few per cent) of the intended $1e\hbar$ quadrupole configuration $[200]_e[220]_h$ is really populated. This is mainly the consequence of using the large detuning. One might be tempted to decreasing the detuning or, alternatively, enhance the population by increasing the laser intensity. But then we would run into the on-linear regime of TDLDA where the cross coupling between numerous states of the system takes place and hence the three-level picture most probably fails. This trouble reflects the more complex dynamics of metal clusters as compared to simple molecules. In any case, even the population of a few percent has to be sufficient to detect the quadrupole state in experiment. The TDLDA calculations for the DTP in Na_{11}^+ showed measurable signatures of the low-lying quadrupole state in PES [10]. A similar situation is expected for the ORSR.

C. ORSR stability

It is still necessary to check the stability of the ORSR scheme to variations of the process parameters. Our tests are illustrated in figure 6. It shows ORSR via the isolated dipole.

The process via the tail of the dipole plasmon (not shown here) produces the same features.

The panels a) of figure 6 show the quadrupole and dipole strengths at larger pulse intensities. The intensities are increased by a factor 3.4 as compared to figure 3. This allows to get a twice stronger quadrupole mode at 0.81 eV. However, we are punished by stronger dipole excitations and a coupling to the quadrupole mode at 2.8 eV (as a part of the quadrupole plasmon), which can complicate discrimination of the target state in PES. So, though the ORSR works even at high intensities, the lower intensities are better suited for the experimental analysis. On the other hand, it is not worth to go below the optimal intensities of figure 3 since this would lead to an unnecessary weakening the quadrupole strength.

The panels b) in figure 6 show that small deviations from the two-photon resonance condition $\omega_p - \omega_s = \omega_2$ lead to weakening of the target mode. Nevertheless, because of the finite width of the mode, the signal does not vanish too rapidly. In fact the width of the mode determines the maximal deviation for ω_s while looking for the mode in the experiment.

Finally, the panels c) of the figure demonstrate what happens without detuning from the intermediate dipole state. In this case, the dipole strength of the intermediate state is considerably increased while the population of the target quadrupole state shrinks. Besides that, a large fraction of competing high-frequency quadrupoles appear. So, a considerable detuning is crucial for the success of the ORSR scheme.

D. DTP exploration of quadrupole plasmon

The top panel of figure 6c deserves a deeper analysis because it demonstrates an important feature of ORSR and similar two-photon processes in metal clusters. Indeed, if two photons from the pump and/or Stokes pulses happen to come into resonance with one of the peaks of the quadrupole plasmon, then this peak is strongly excited. Such a case is observed in the top panel of figure 6c). Comparison of this plot with Fig. 2 shows that $2\hbar\omega_p = 2.7$ eV and $2\hbar\omega_p + 2\omega_s = 3.7$ eV: this approximately covers two of the plasmon states and thus result in two prominent pikes at these energies. Obviously, such undesirable excitation of the quadrupole plasmon can spoil the discrimination of low-frequency quadrupole modes in PES. At the same time, this provides new possibilities for simultaneous investigation of low- and high-frequency quadrupoles.

The example above indicates that implementation of two lasers with different frequencies

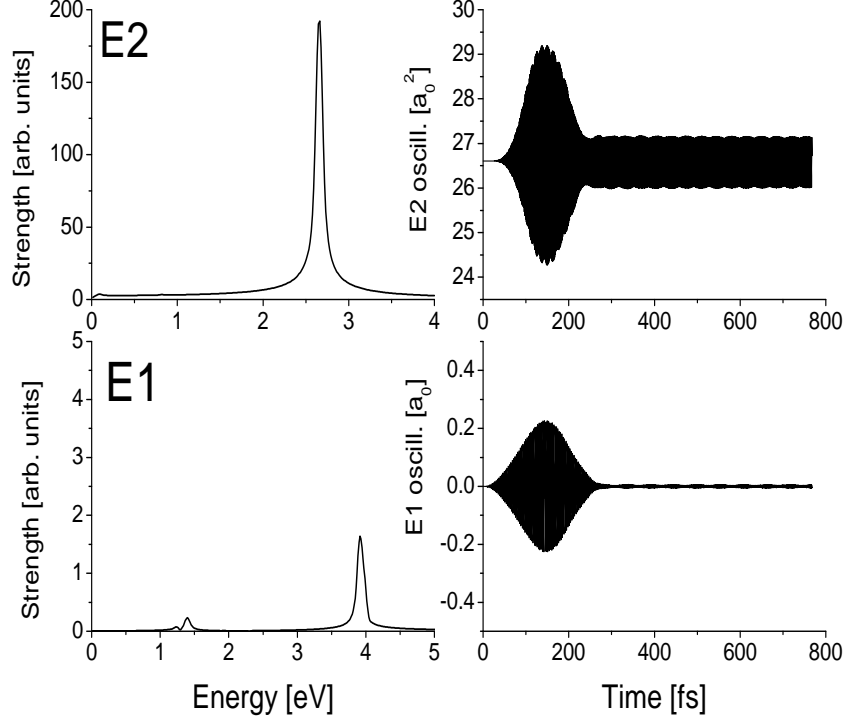


FIG. 7: Direct two-photon excitation of the quadrupole plasmon state at 2.6 eV in Na_{11}^+ . The cluster is irradiated by the pump laser only, with characteristics $\hbar\omega_p = 1.31$ eV, $I_p = 2.2 \cdot 10^{10} \text{ W/cm}^2$ and $T_s = 300$ fs.

complicates the analysis of the quadrupole plasmon because we may have at once more than one resonance. This would hinder the detection procedure. For the same reason is not optimal to use for investigation of high-frequency states the ORSR in the ladder configuration. It is much better to apply the DTP method proposed in [10], where the quadrupole state of interest is populated by absorption of two photons from one laser, as shown in figures 1 and 2. An example of such a DTP process is presented in figure 7 where the resonant absorption of two photons from the pump laser results in a strong excitation of the quadrupole plasmon state at 2.6 eV. Unlike the top panel of Fig. 6c), only one frequency is involved and thus only one resonant peak excited. A properly tuned DTP with scanning frequencies allows to investigate the quadrupole plasmon state by state.

E. Proposed experiment

The discussion above shows that the most optimal way is a simultaneous investigation of the low- and high-frequency quadrupole states by a combination of ORSR and DTP

methods, respectively. For this aim we need three synchronized lasers: tunable infrared pump and Stokes lasers and ultraviolet probe laser.

The detection scheme can be the same as proposed in [10]. Namely, the cluster is irradiated by a probe pulse (with an appropriate delay) leading to a direct emission of electron out of the excited quadrupole state. The coupling of the quadrupole oscillation to the single-electron PES structures will create the satellites in the PES. Thus, by recording the PES and measuring the relative frequencies of the satellites, one may determine the frequency of the quadrupole state.

The experiment should follow three steps.

1) As a first step, we should find the optimal parameters (intensity, duration, ...) for the probe pulse responsible for the photoionization of the cluster and detection process. For this aim we should scan the pulse parameters so as to get the strongest and, at the same time, distinct single-particle PES from the ground state. Our predictions [10] for the optimal pulse intensities and durations ($I = 2 \cdot 10^{10} - 2 \cdot 10^{11} W/cm^2$ and $T = 200 - 500$ fs) can be used here as a first guess. These predictions are relevant for all three pulses (pump, Stokes and probe) which may have similar characteristics, apart from the photon frequency.

In principle, the photoionization can be also provided by the coherent synchrotron source with high-frequency photons. Then the two-photon ionization proposed in [10] can be replaced by more effective one-photon ionization. In this case, the characteristics of the pump and Stokes pulses can be taken again from [10], while the parameters of the probe irradiation need an independent adjusting.

2) Now we can proceed with the next step: to explore the high-frequency states of the quadrupole plasmon. We use here only the pump and probe lasers. The pump frequency is scanned until its double value comes into resonance with the states of the quadrupole plasmon. The probe pulse should have sufficient delay with respect to the pump pulse so as to be safely decoupled from it and to measure self-sustaining oscillations only. Since the quadrupole plasmon has high energy, one-photon ionization by a probe laser in the visible range suffices for our aims. The maximum satellite signal provides the quadrupole energy in two ways, first as the double pump frequency and second (as a countercheck) from the offset of the satellites. Thus one can explore, state by state, all the quadrupole plasmon [26].

3) In a final step, one can refine the measurement of the low-frequency quadrupole state. First, one should choose the optimal intermediate dipole frequency by combining a suitable

detuning above or below the dipole state with the feature that the double pump frequency lies between the peaks of the quadrupole plasmon and thus avoid their resonance excitation. By such a way we will hopefully minimize the influence of the quadrupole plasmon. Then one should scan the Stokes laser until the two-photon resonance $\omega_p - \omega_s = \omega_2$ with a low-frequency quadrupole is achieved.

The proposed scheme allows to obtain not only the frequencies of the quadrupole states but also their lifetime. To that end, one should simply increase, step by step, the delay between the pump and probe pulses. The relaxation of quadrupole oscillation will finally lead to an extinction of the satellites from which one can read off the lifetime.

IV. CONCLUSIONS

In this paper, we have proposed a combined exploration of electronic quadrupole low-frequency (infrared region) and high-frequency (region of the quadrupole plasmon) states in free metal clusters by means of two-photon processes: direct two-photon (DTP) excitation and off-resonant stimulated Raman (ORSR) scattering. The DTP uses one pump laser and retrieves the two photons from it while the ORSR employs a pump and a Stokes pulses with different frequencies. The final proof of the successful excitation of a quadrupole mode is achieved by a probe pulse with a subsequent measurement of the photo-electron spectra (PES). The present analysis is based on realistic simulations within the time-dependent local density approximation. The main attention is paid to the ORSR which, for our knowledge, still have never been considered for atomic clusters.

The calculations show that the high-frequency quadrupole states in the regime of the quadrupole plasmon are preferably explored by DTP. The more flexible ORSR is a powerful tool to investigate the isolated low-frequency (infrared) quadrupoles. ORSR allows to use various intermediate dipole states, from the isolated infrared dipoles to the dipole plasmon. In all the cases, an appreciable detuning from true dipole states is crucial to avoid unwanted cross talk. A proper combination of both methods (DTP, ORSR) should allow to explore both spectra and lifetimes of the quadrupole states. We have worked out optimal parameters of DTP and ORSR schemes and checked the sensitivity of the schemes to parameter variations. The proposed two-photon schemes are quite general and, in principle, can be used for a variety of clusters including supported and embedded ones.

The low- and high-frequency quadrupole states can deliver important information on electron-hole excitations inside the valence shell ($\Delta N = 0$) and through two shells ($\Delta N = 2$). By combining the two-photon and photoelectron data, one can get the single-electron energies above the Fermi level and thus greatly enlarge our knowledge on the mean field spectra of valence electrons. These spectra give access to other cluster features (mean field, deformation) and provide a critical test for the theory of cluster structure.

Acknowledgments

V.O.N. thanks Profs. K. Bergmann and B.W. Shore for valuable discussions. The work was partly supported by the DFG grant GZ:436 RUS 17/104/05, the grant of University of Paul Sabatier (Toulouse, France) and Heisenberg-Landau (Germany-BLTP JINR) grants for 2005 and 2006 years.

References

-
- [1] P.-G. Reinhard and E. Suraud, *Introduction to Cluster Dynamics*, (Wiley-VCH, Berlin, 2003).
 - [2] G. Wrigge, M. Astruc Hoffmann and B.v. Issendorff, *Phys. Rev. A* **65**, 063201 (2002).
 - [3] M. Moseler, B. Huber, H. Häkkinen, U. Landman, G. Wrigge, M. Astruc Hoffmann and B.v. Issendorff, *Phys. Rev. B* **68**, 165413 (2003).
 - [4] J. Akola, M. Manninen, H. Hakkinen, U. Landman, X. Li, and L.-S. Wang, *Phys. Rev. B* **60** R11297 (1999).
 - [5] L. Kronik, R. Fromherz, E. Ko, G. Ganteför, and J.R. Chelikovsky, *Nat. Matter*, **1**, 1 (2002).
 - [6] M.E. Madjet, H.S. Chakraborty, and J.-M. Rost, *J. Phys. B: At. Mol Opt. Phys.* **34**, L345 (2001).
 - [7] E.E.B. Campbell, K. Hansen, K. Hoffmann, G. Korn, M. Tchapyguine, M. Wittmann, and I.V. Hertel, *Phys. Rev. Lett.* **84**, 2128 (2000).
 - [8] E.E.B. Campbell, K. Hoffmann, H. Rottke, and I.V. Hertel, *J. Chem. Phys.* **114**, 1716 (2001).
 - [9] V.O. Nesterenko, P.-G. Reinhard, W. Kleinig and D.S. Dolci, *Phys. Rev. A* **70**, 023205 (2004).

- [10] V.O. Nesterenko, P.-G. Reinhard, Th. Halfmann, and L.I. Pavlov, *Phys. Rev. A* **73**, 021201 (2006).
- [11] *Atomic and Molecular Beam Methods*, ed. G. Scoles, (Oxford Univ. Press, Oxford, 1988).
- [12] *Molecular dynamics and spectroscopy by stimulated emission pumping*, ed. H.-L. Dai and R.W. Field (Advanced series in physical chemistry, **4**, World Scientific, Singapore, 1999).
- [13] N.V. Vitanov, M. Fleischhauer, B.W. Shore, and K. Bergmann, *Adv. Atom. Mol. Opt. Phys.*, **46**, 55 (2001).
- [14] K. Bergmann, H. Theuer, and B.W. Shore, *Rev. Mod. Phys.* **70**, 1003 (1998).
- [15] V.O. Nesterenko, P.-G. Reinhard, W. Kleinig, ArXiv: physics/0512061.
- [16] F. Calvayrac, P.-G. Reinhard, E. Suraud, and C.A. Ullrich, *Phys. Rep.* **337**, 493 (2000).
- [17] J.P. Perdew and Y. Wang, *Phys. Rev. B* **45**, 13244 (1992).
- [18] C. Legrand, E. Suraud and P. G. Reinhard, *J. Phys. B: At. Mol. Opt. Phys.* **35**, 1115 (2002).
- [19] M. Brack, *Rev. Mod. Phys.* **65**, 677 (1993).
- [20] W.A. de Heer, *Rev. Mod. Phys.* **65**, 611 (1993).
- [21] B. Montag, Th. Hirschmann, J. Meyer, P.-G. Reinhard, and M. Brack, *Phys. Rev. B* **52**, 4775 (1995)
- [22] F. Calvayrac, E. Suraud, and P.-G. Reinhard, *Ann. Phys.* **254** (N.Y.), 125 (1997).
- [23] K. Clemenger, *Phys. Rev. B* **32**, R1359 (1985).
- [24] In principle, the quadrupole plasmon can be also explored by the ORSR in the ladder configuration when the successive levels lie higher than the predecessors. However, as is shown in the subsection 3.4 this option is not optimal.
- [25] A. Pohl, P.-G. Reinhard, and E. Suraud, *J. Phys. B: At. Mol. Opt. Phys.* **34**, 4969 (2001).
- [26] The pump frequency can accidentally coincide with one of the isolated dipole states below the dipole plasmon and thus result in the additional PES satellites. However, these satellites can be easily recognized through a slight shift of the probe frequency, see [25] for more details.